ITER Divertor Relevant Plasma Achieved in the Magnum-PSI Programme.

N.J. Lopes Cardozo[1,2], G.J. van Rooij[1], V.P. Veremiyenko[1], R.S. Al[1], M. Baeva[1], S. Brons[1], R. Engeln[2], H.J.N. van Eck[1], W.J. Goedheer[1], B. de Groot[1], A.W. Kleyn[1,3], R. Koch[4], W.R. Koppers[1], H.J. van der Meiden[1], V. Philipps[5], M.J. van de Pol[1], P.R. Prins[1], E.D. de Rooij[1], U. Samm[5], J. Scholten[1], D.C. Schram[1,2], B. Schweer[5], P.H.M. Smeets[1], W.A.J. Vijvers[1], J. Westerhout[1], D.G. Whyte[6].

[1]FOM Institute for Plasma Physics Rijnhuizen, Ass. Euratom-FOM, TEC, Nieuwegein, The Netherlands, www.rijnhuizen.nl; [2]Eindhoven University of Technology, The Netherlands; [3]Leiden University, The Netherlands; [4]ERM/KMS, Ass. Euratom-Belgian State, TEC, Belgium; [5]Forschungszentrum Jülich, Inst. für Plasmaphysik, Ass. Euratom-FZJ, TEC, Jülich, Germany. [6] MIT, Cambridge, USA.
e-mail address: cardozo@rijnh.nl

Abstract
The PSI-laboratory at FOM-Rijnhuizen includes linear plasma generators reaching the ITER relevant strongly coupled limit of PSI and a surface analysis station. The largest plasma generator, Magnum-PSI, designed to provide a 10 cm diameter beam delivering <10 MW/m^2 power to a target at typically T_e=1-5 eV and n_e<10^{21} m^{-3}, is presently under construction. A smaller prototype, Pilot-PSI is operational and has achieved record plasma parameters of n_e<4.10^{21} m^{-2}s^{-1} with T_e=1-5 eV, in a 1 cm wide beam confined by B<1.6T. The plasma source used in these experiments is a cascaded arc. At 17 mm from the target (0.5 m distance from the source), n_e>10^{21} m^{-2}s^{-1} with T_e>1 eV have been measured with Thomson scattering. Initial experiments on erosion of fine-grain carbon samples showed that up to 20 µm/s could be eroded. Numerical simulations with the B2-Eirene code confirm that in Magnum-PSI a 'detached divertor'-like condition will very likely be achieved.

1. Introduction.

Plasma surface interaction (PSI) in the divertor of ITER and fusion reactors beyond ITER is a critical research area in the development of fusion power. For ITER, power and particle flux densities of 10 MW/m^2 and 10^{24} m^{-2}s^{-1}, respectively, are foreseen, at n_e < 10^{21} m^{-3} and T_e in the 1-5 eV range [1-2]. To address the physics of PSI in this extreme parameter regime, FOM, in collaboration with its TEC partners and as part of the Euratom fusion programme, is building an integrated PSI laboratory [3]. The PSI-lab includes the high-flux linear plasma generator Magnum-PSI and its smaller fore-runner Pilot-PSI. These will provide steady state ITER relevant fluxes at B<3 T, with high accessibility to exposed surfaces. The design goals of Magnum-PSI are: steady state operation of plasma source with B<3 T, plasma beam diameter up to 10 cm, flux density < 10^{24} m^{-2}s^{-1} at T_e=T_i in the eV range, density in front of target up to or exceeding 10^{21} m^{-3} [4]. The cooled target can be placed under a small angle with the plasma beam and can be retracted in a surface analysis station. Extensive diagnostics will include *in situ* Sum Frequency Generation to study surface processes in real time. Plasma diagnostics include probes, Thomson scattering, high-resolution emission spectroscopy, laser induced fluorescence cavity ringdown absorption spectroscopy, and high-speed imaging diagnostics. The plasma generators are combined with a surface analysis laboratory, which includes SEM, XPS, and Auger spectroscopy.

In parallel to the experimental programme a numerical modeling programme is being developed. The modeling of the plasma physics, specialized to the linear plasma generators but in a more generic context, is approached along different lines, with well-established codes including B2-Eirene [5,6], the DS2V Direct Simulation Monte Carlo Code, the VAC-code (MHD), a PIC/MC approach (plasma expansion and dust behaviour) and the PLASIMO code (for the plasma production in the cascaded arc source). For near-surface interactions, EIRENE and the MD5 molecular dynamics code are used. Together, these approaches seek to provide an integrated approach from the edge plasma to the material surfaces. The approach is sufficiently generic that links to related fields – astrophysical jets, industrial plasmas, dusty plasmas – are maintained. The well-diagnosed PSI experiments will serve to benchmark the numerical models and generalize the results.

This paper introduces PSI-lab, with emphasis on the breakthrough in magnetized plasma beam generation achieved in Pilot-PSI and first experiments on erosion of fine grain carbon targets.

2. PSI-lab – an overview.

Figure 1 gives an overview of the PSI-lab. Magnum-PSI is the high flux, linear plasma generator with superconducting coils; it is combined with the plasma diagnostics and in-situ surface diagnostics (SFG=Sum-Frequency Generation), ex-situ, in-vacuo surface analysis station, and the existing Pilot-PSI plasma generator. Thin Film PSI is an advanced coater used for research aimed at the development of highly resilient XUV optics. It is connected under UHV with an X-ray Photoelectron Spectrometer (XPS), Secondary Electron Microscope (SEM) and a Scanning Tunneling Microscope (STM; under construction). The Surface-PSI experiment is a UHV plasma-surface interaction device to study elementary plasma surface interaction processes at the surface at very low flux. Samples from Magnum-PSI can be analysed in the analysis station while vacuum is maintained. Transportation to the XPS station at a distance of 50 m from Magnum-PSI can be done under controlled atmosphere. The analysis station is connected – *in vacuo* – with a custum-built advanced coater, in which thin films can be deposited. This device is used for an industrial research programme, as well as for the preparation of samples for erosion experiments in Pilot-PSI and Magnum-PSI.

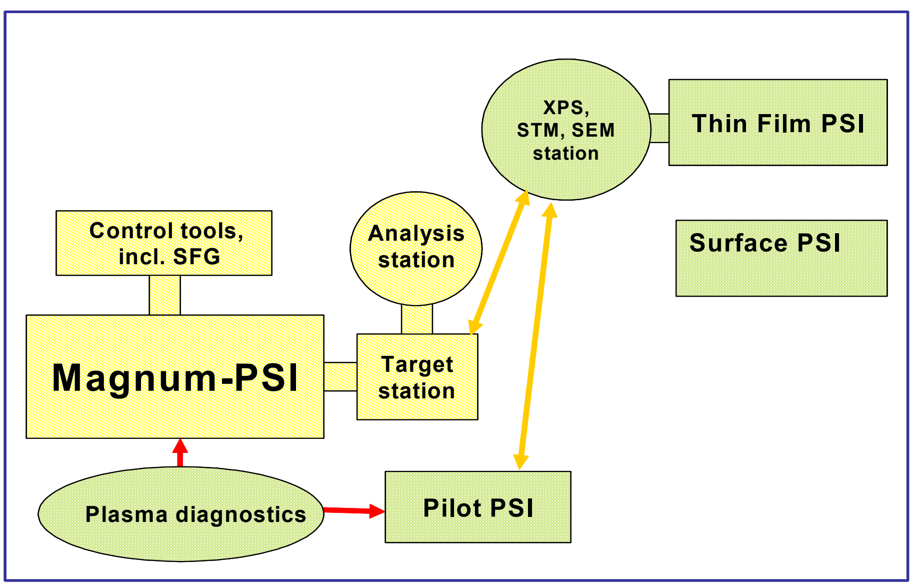

Figure 1. Schematic of PSI-lab. The green elements are already operational; the yellow elements are under construction. See text for explanation.

3. ITER-divertor grade plasma achieved in Pilot-PSI.

Pilot-PSI consists of a 1 m long 0.4 m diameter vacuum vessel (≈0.1 Pa background pressure) placed inside five coils that produce a pulsed axial magnetic field up to 1.6 T (CW at 0.2 T, 10 s pulse length at 1.6 T). The plasma source is a cascaded arc [7], which exhausts into the vessel along the magnetic field axis. It consists of three tungsten cathodes in a cathode chamber, a stack of 5 separately insulated water cooled copper plates with a 4 mm hole that form a 30 mm length discharge channel, and a copper-tungsten nozzle that also serves as anode. Figure gives the schematics of source and plasma generator. The source was operated on hydrogen with a gas flow of 2.5 slm = 1.1×10^{21} H_2/s and a discharge current of 100 A. This sets the cathode chamber pressure to 10^4 Pa. Due to the high densities at elevated pressure, the temperature is more or less fixed at kT ≈ 1.3 eV in the source. At the exit of the plasma channel the plasma flows at sound speed (Mach = 1 boundary condition) and expands into the vessel. Profiles of n_e and T_e were measured with Thomson scattering at 40 mm from the nozzle (i.e. well outside the source). The scattered light was collected with an array of fibers to obtain radial profiles over an observational chord of 25 mm.

The photograph in Fig.3 gives an impression of the bright hydrogen plasma beam that reaches the target at approx. 80 cm distance from the source. Figure 4 gives a typical result of Thomson scattering measurement at 40 mm from the nozzle. For the source at hand densities in excess of 7×10^{21} m^{-3} were reached with T_e around 1.5 eV. The T_e profiles are in all cases wider than the n_e profiles. To determine the flux density in the plasma beam, the Doppler shift of the H_β-line was measured with high-resolution emission spectroscopy, using a small viewing angle with respect to the axis. v_{axial} = 3.5 km/s was found at 40 mm from the nozzle for all field settings. Line profiles were also measured for a perpendicular viewing line to determine the ion temperature and plasma rotation velocity.

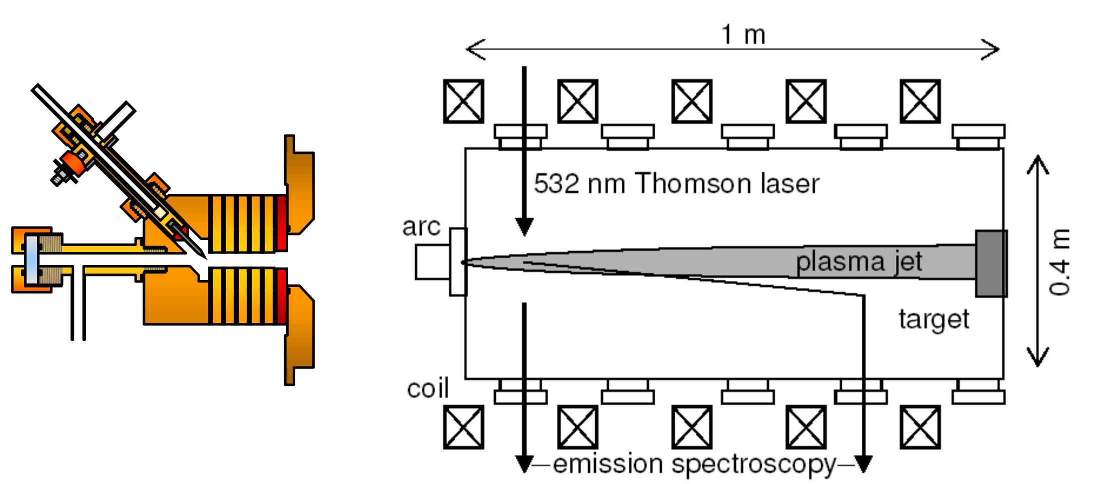

Figure 2. Schematic of the Pilot-PSI plasma generator and blow-up of the cascaded arc source..

Figure 3. A beam of hydrogen plasma in the Pilot-PSI linear plasma generator. On the left-hand-side is the cascaded arc source. The beam reaches the target on the right-hand-side at 0.8 m from the source.

After optimization of the source, peak values of n_e in excess of 7×10^{20} m^{-3} were measured at T_e=1.5 eV, at 40 mm from the nozzle. (See Fig.4). The peak density increases linearly with B, T_e is independent of B. It was found that especially the shape of the nozzle of the source is of importance for the efficiency of plasma production. For a wide nozzle, fast camera images showed that the current protrudes outside the arc before returning to the nozzle. This would result in effective Ohmic heating of the plasma just outside the nozzle, where there is no loss due to interaction with the channel wall.

Using the source with a wide nozzle in combination with a 1.6 T magnetic field, net ionization efficiencies of 16% have been achieved (i.e. the fraction of the hydrogen fed into the source that is found as H^+-ions at 40 mm from the nozzle).

Spectroscopic measurements show that Ti≈Te and that the beam is rotating fast, reaching sound speed. This requires a strong radial electric field, in agreement with the observed Ohmic heating. Whether the fast rotation could give rise to viscous ion heating needs to be investigated further.

In recent experiments the channel width has been increased up to 7 mm, discharge currents up to 300 A, while the gas flow was reduced down to 0.2 slm in extreme cases. In this way T_e > 4 eV and n_e> 4×10^{21} m^{-3} have been measured at 40 mm from the nozzle. Preliminary results of Thomson scattering measurements taken at 17 mm from the target, ≈ 0.5 m distance from the source, showed that here n_e> 1.5 10^{21} m^{-3} has been realised at T_e ≈ 1.7 eV. In those cases no current was drawn to the target (which was at floating potential). By drawing an electron current to the target, T_e>4 eV has been measured at n_e ≈ 10^{20} m^{-3}. T_e and n_e at the target depend sensitively on B and the current in the cascaded arc source, which thus provide an excellent control over the plasma conditions at the target.

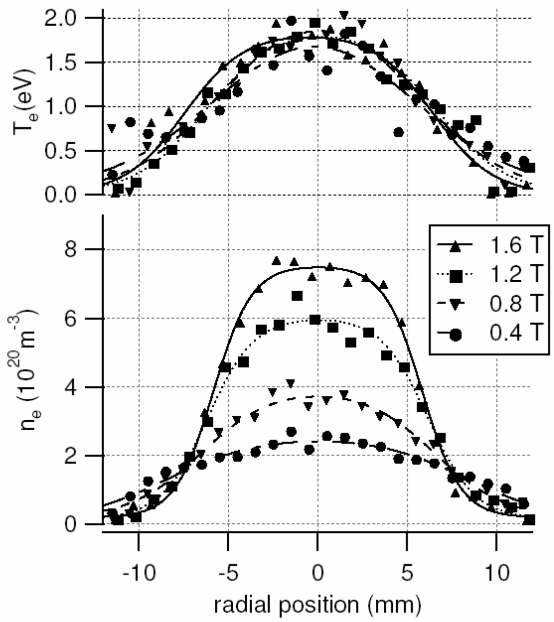

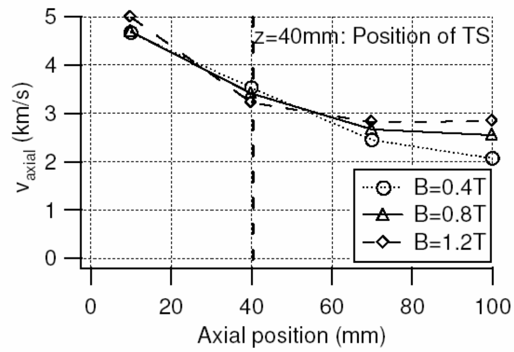

Figure. 4. Thomson scattering measurements taken 40 mm from the source, showing electron density and temperature profiles for different values of the axial magnetic field, for moderate source parameters: 4 mm bore, 100 A discharge current, 2.5 slm H_2 gasfeed. The lower panel gives the measurement of the forward velocity of the plasma. These densities, temperatures and flow velocity, and the associated particle and energy flux density, bring the Pilot-PSI plasma source in the regime that allows erosion experiments in conditions relevant to the ITER divertor.

4. First results on erosion of carbon targets in Pilot-PSI

First results have been obtained with exposure of carbon targets to the Pilot-PSI plasma beam. The samples consisted of discs of fine–grain carbon with a diameter of 26 mm and a thickness of approx. 2.4 mm. The samples were clamped on a water-cooled heat sink. The target was placed at 54 cm from the nozzle of the plasma source. The three exposures discussed here were carried out with a cascaded arc source with a 7 mm bore channel, the axial magnetic field set to 0.4 T, with a typical exposure time of 100 s. The discharge current in the source was 100 or 180 A. The gas flow to the source was set at 0.2 or 0.5 slm, resulting in a neutral pressure in the vessel of 0.5 and 1.6 Pa, respectively.
The target was grounded in these experiments, i.e. at the same potential as the nozzle of the source. Depending on the conditions, an electron current to the target was measured of up to 59 A, the highest currents being found at the lowest neutral pressure.
The profiles of n_e and T_e were measured by Thomson scattering at 40 mm from the nozzle.
The net power to the target was measured by calorimetric measurement of the cooling water.
In similar conditions, Thomson scattering measurements of n_e and T_e were taken close to the target, at 17 mm from the surface. During exposure visible light spectroscopy was used to estimate the surface temperature. After exposure, the targets were analysed using SEM, and Auger spectroscopy. The depth profile of the eroded spot was measured with a mechanical gauge. Table 1 summarizes the conditions and measurements of the 3 samples. Figure 5 shows a photograph and the depth profile of sample 3, Figure 6 typical SEM images.

Table 1. Conditions and results of erosion experiments for 3 fine grain carbon samples, exposed to the Pilot-PSI plasma beam for 100 s.

.

Sample	P_{vessel} [Pa]	I_{sample} [A]	N_e (at 40 mm) [10^{20} m^{-3}]	T_e (at 40 mm) [eV]	Ptarget [W]	$D_{erosion}$ [mm]	ΔM [mg]
1	1.6	47	2.0 ± 0.1	3.8 ± 0.2	425	1.1	11
2	1.6	24	2.5 ± 0.3	4.2 ± 0.5	400	0.1	1
3	3.5	59	1.6 ± 0.1	4.2 ± 0.3	530	2.0	41

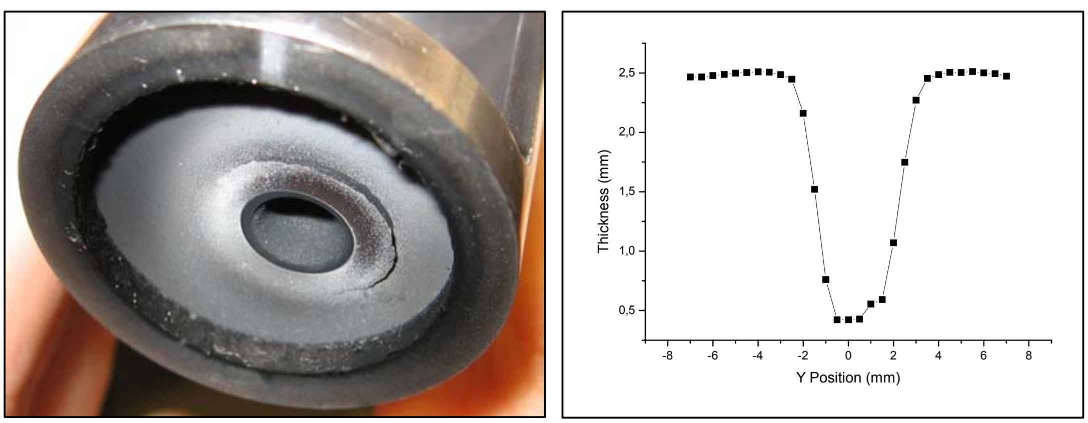

Figure 5. Photograph and depth profile of sample 3.

The following qualitative observations were made on the target erosion itself:

1. a spot with a diameter of about 6 mm is eroded
2. the spot is near perfectly circular and has a sharply defined edge
3. around the eroded spot, a wider area is observed with deposition to a maximum thickness of 60 μm.

4. the rate of erosion depends strongly on conditions and can reach very high values: in sample 3, 41 mg of fine-grain carbon, i.e. a thickness of 2 mm, was eroded in 100 s.
5. Auger analysis of the sample does not show any traces of Cu, W or other impurities that could have come from the source.

The mechanism for the very fast erosion is presently under study. Pure chemical erosion is not physical as an explanation, it would require an erosion coefficient of Y=0.6.
Several mechanisms, including anode spot formation and radiation enhanced sublimation, are considered. Based on the spectroscopic measurement the surface temperature during erosion is estimated at 1700 C, assuming that the temperature of the eroded area is uniform. If the heating is more localised, a higher value of T would be deduced. Spectroscopic measurements do show the formation of CH, indicating that chemical erosion does play a role in the process.
The overall conclusion of these experiments is that in Pilot-PSI the heat flux to the target and plasma conditions can be achieved that are in the range that is relevant for tokamak divertors. The conditions are well controlled, with the B-field, the current in the cascaded arc, the current to the target and the neutral pressure in the vessel as the main experimental knobs. The beam in Pilot-PSI is too narrow to allow for effective recycling, although a limited amount of redeposited material is found around the strike area.

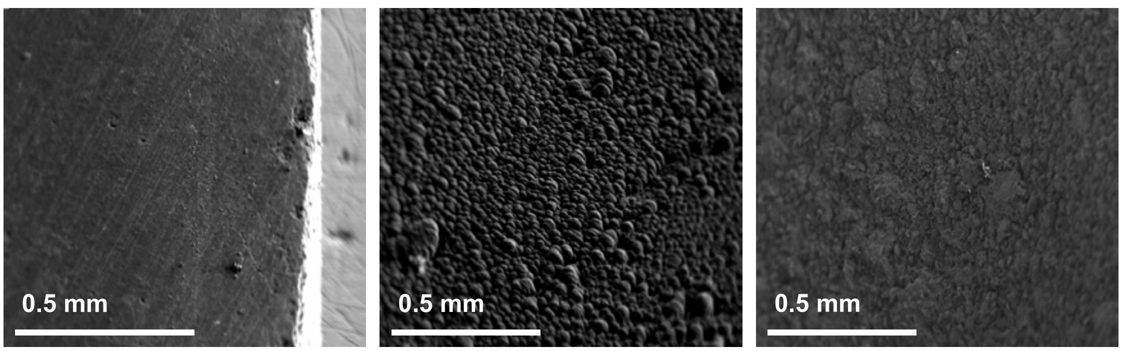

Figure 6 .SEM photographs of sample 3. From left to right: unaffected edge of the sample, exposed area and the center of the crater.

5. Development of Magnum-PSI

The Magnum-PSI device is in the stage of detailed design. An impression of the apparatus is given in the figure. For the plasma source, an upscaled version of the cascaded arc source used in Pilot-PSI will be used. Scaling studies indicate that power efficiencies in excess of 10% can be expected. Pressure control is achieved by three stage differential pumping, using roots pumps to pump the large influx of neutral hydrogen. The superconducting magnet has been predesigned. It will have a bore of 1.3 m and a length of 2.5 m, and two times 8 room temperature diagnostic ports. It will be placed on rails so that it can be moved to allow access to the vacuum vessel. This consists of three elements that can be modified if necessary. The exposure chamber has been designed for optimal diagnostic access. Figure 7 presents an artist's impression of the device. The target has a width of 10 cm and a length of 60 cm, can be tilted to allow grazing incidence, rotated and axially translated, and will have 100 kW cooling capacity. It can be retracted into a target analysis chamber, in which samples can be mounted and dismounted and where a first surface analysis can be performed. Like in Pilot-PSI, plasma heating will be provided by Ohmic dissipation (by drawing a current either to the target or to a ring electrode) and RF heating. The project aims at first plasma early 2009.

.

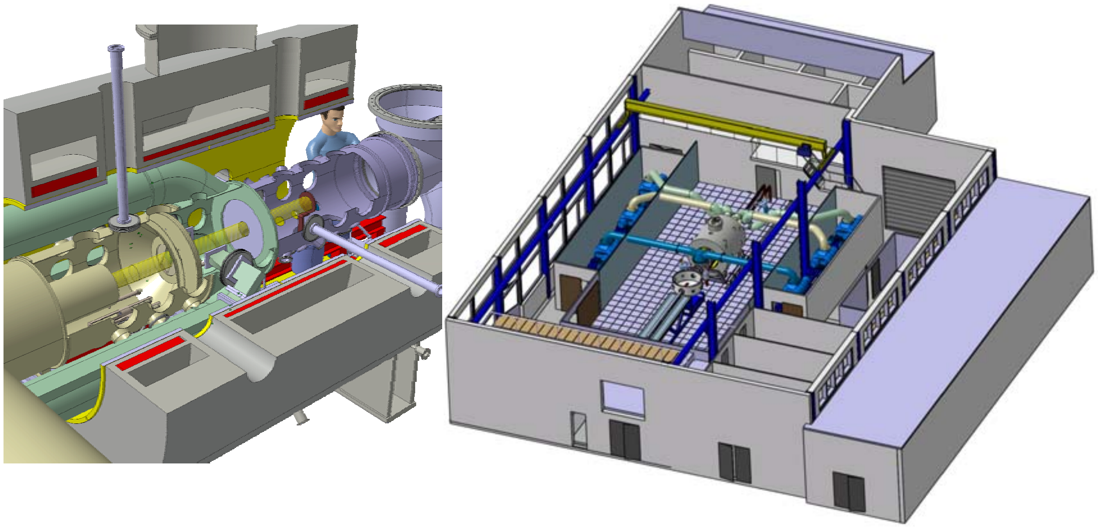

Figure 7. Artist's impression of the Magnum-PSI linear plasma generator, showing the three differentially pumped vacuum chambers, separated by skimmers. The first chamber is heavily pumped to remove most of the neutral gas produced by the source. The second chamber will have a low neutral pressure and is dedicated to rf-heating of the beam. The third chamber, in which the plasma interacts with the target, is narrower and has many ports to allow maximum diagnostic access. The plasma beam is stopped by a beam dump in this picture, the target is retracted into the target analysis chamber. On the right an overview of the experimental hall in which Magnum-PSI will be constructed. Clearly visible are the large roots pumps and pumping ducts..

6. Integrated modeling – results of B2-Eirene simulations of Magnum-PSI.

The B2-EIRENE code simulates the plasma (B2) and its interaction with neutral species (EIRENE). Topics addressed are Molecule Assisted Recombination (MAR) induced by vibrationally excited H_2 molecules, detachment of the plasma from the substrate. Gas puffing can be applied at the inlet, simulation gas coming from the source, and at the target.

Typical T_e profiles along the axis are shown in Fig. 8. At the inlet, i.e. in the second (heating) chamber of Magnum-PSI, T_e is put at 12 eV, as a boundary condition to realise the power flux density of 10 MW/m^2. T_i is 2 eV at the inlet, but quickly equilibrates and becomes equal to T_e after about 0.2 m.

In all simulations an ionization front is generated in front of the target, where the plasma density decays rapidly and the neutral density rises. Detached plasmas are thus generated, in which the heat flux is to a large extent lost in ionization of recycling neutrals.

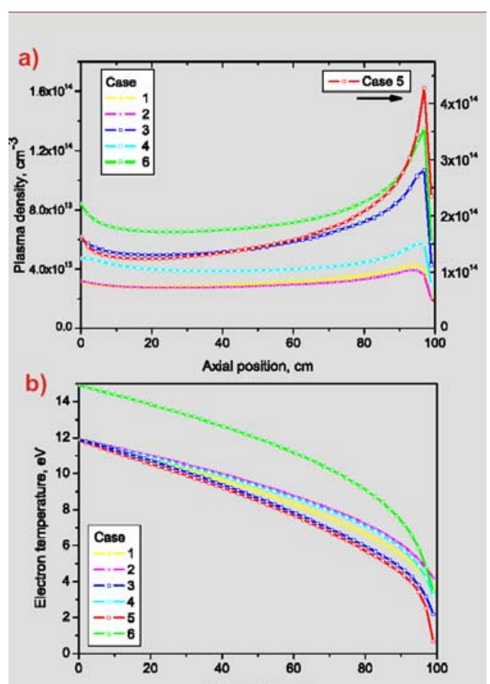

Figure 8 Axial profiles of T_e and n_e computed with B2-Eirene.

Examples in Fig. 8 show a steep increase of the plasma density due to the drop in temperature and the above mentioned fast decay toward the target. Neutrals puffed in at the inlet, with a rate of a few slm, are easily taken up by the plasma and ionized, showing the effect of plasma plugging. Thus, the neutral pressure near the target totally originated from the neutralization of plasma species. The beam diameter, taken as 10 cm at the inlet, remains approximately constant over the whole length of the simulation domain.

7. Conclusion

In conclusion, experiments in Pilot-PSI show that densities and temperatures of ITER divertor relevance can be realised at the target. Erosion experiments confirm that that fast erosion can be achieved. These results validate the concept of using the cascaded arc as an efficient hydrogen plasma source and the feasibility of confining and transporting that beam with the help of a strong magnetic field. Pilot-PSI itself – albeit with a narrow plasma beam that does not give access to the strongly coupled regime in which redeposition is important – reaches flux densities and plasma conditions close to those foreseen for the ITER divertor.

Acknowledgement

This work, supported by the European Communities under the contract of Association between EURATOM and FOM, was carried out withing the framework of the European Fusion Programme with financial support from NWO.

References.

[1] ITER Physics Basis Editors, Nucl. Fusion 39, 2137 (1999).

[2] G. Federici, et.al, Nucl. Fusion, 41, 1967 (2001); G. Federici, et.al, J. Nucl. Mater., 313-316, 11 (2003).

[3] A.W. Kleyn, N. J. Lopes Cardozo, and U. Samm, Phys. Chem. Chem. Phys. 8, 1761 (2006).

[4] B. de Groot, et.al, Fusion Eng. Des. 74, 155 (2005);

[5] B. J. Braams, 'Computational studies in Tokamak Equilibrium and Transport', PhD Thesis, University of Utrecht (1986);

[6] D. Reiter, M. Baelmans, P. Brner, 'The EIRENE and B2-EIRENE codes', Fus. Sci. Techn. 47-2 (2005) 172.

[7] M. C. M. van de Sanden, J. M. de Regt, G. M. Janssen, J. A. M. van der Mullen, D. C. Schram, and B. van der Sijde, Rev. Sci. Instrum. 63, 3369 (1992).